

Application of the van der Pauw technique in characterising the carrier properties of InSb, n-type and p-type doped GaAs

Thomas Fahey
Department of Physics
Imperial College London
Blackett Laboratory
London SW7 1AZ U.K.

December 15, 2017

Abstract

The carrier mobility (μ) and density (n) for Indium Antimonide and n-type and p-type Gallium Arsenide were investigated using the van der Pauw technique, for thin samples with approximately square geometry. The Hall voltage and sheet resistance were measured under linearly varying current and magnetic induction conditions, from which the effective Hall coefficient for the samples was derived. The calculated values for μ and n were compared to the literature and the relative error due to the sample's contact size/placement explored, suggesting a more accurate measurement could be achieved with more precisely fabricated samples.

1 Introduction

The macroscopic properties of semiconducting materials are of considerable interest today; with the annual number of semiconductor unit shipments forecast to exceed 1 trillion devices this year ¹, there is an ever-growing demand for new microelectronic devices utilising the seemingly inexorable supply of applicable phenomena associated with semiconductors.

Two fundamental parameters of semiconductors are their carrier densities, n and mobilities μ . The mobility measures the “ability of free carriers (electrons or holes) to move in the material as it is subjected to an external electric field...” - a crucial parameter in semiconductor device operation, as it directly determines properties such as “...operation speed through the transit time across the device...circuit operating frequency, or the sensitivity in magnetic sensors...” [3] in electronic devices, “charge extraction and recombination dynamics” in organic solar cell materials [2] amongst many others. The carrier mobility and density together determine the conductivity of a semiconductor, an incredibly important factor in the design of low power, efficient electronics, but also a principle which has been exploited to great effect on the problem of gaseous-state chemical detection, in the design of semiconductor gas sensors (see [10, 1]).

The ability to accurately measure the carrier mobility and density is therefore of enormous significance in the use of semiconductor devices. In this lab experiment, the carrier mobility and density for three semiconductor samples were obtained via measurement of their effective Hall coefficient, consisting of one non-doped sample of Indium Antimonide (InSb) and two doped samples of Gallium Arsenide (GaAs), one n-type, the other p-type.

2 Theory

2.1 Hall Effect

The Hall effect is often cited as the most well known example of a more general set of phenomena called galvanomagnetic effects which, as the name suggests, describe “the action of the Lorentz force on quasi-free charge carriers in condensed matter” [7], which takes the form:

$$\vec{F}_{Lorentz} = q\vec{E} + q(\vec{v} \times \vec{B}) \quad (1)$$

where the first term on the right describes the force experienced by the charge carriers, due to an electric field \vec{E} and the second term, that due to the motion of the charges through a magnetic field \vec{B} .

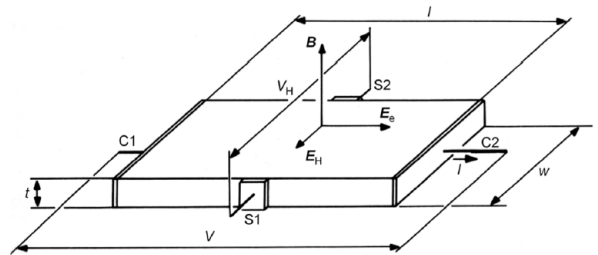


Figure 1: Schematic of the potential induced as a result of a magnetic field acting on a thin plate conductor (see [7])

If we consider the geometry of a thin square plate (Figure 1) with current \vec{I} sourced at C1 and sunk at C2 flowing in one direction through it and an external magnetic field directed perpendicular to the surface of the plate; from equation 1, it can be seen that: the current is driven in one direction along the plate by an applied electric field, \vec{E}_e , from C1 to C2, and that; the magnetic component of the Lorentz

¹The McClean Report, IC Insights Inc.

force causes a deflection of the current in the direction diametrically opposite to it, towards S1. The accumulation of charge at S1 leads to an increasing potential which, at steady state, produces an opposing electric field, $\tilde{\mathbf{E}}_H$, which exerts a force on the charge carriers exactly equal to the deflecting force:

$$q\tilde{\mathbf{E}}_H = q(\tilde{\mathbf{v}} \times \tilde{\mathbf{B}}) \quad (2)$$

The potential at steady state, which can be readily measured by application of sense contacts at S1 and S2, is referred to as the Hall voltage, V_H .

The crucial aspect of this effect is that it depends on a microscopic property of the conducting material, namely, $\tilde{\mathbf{v}}$, the velocity of the moving charges that make up the current. This itself is related to the applied electric field driving the current, by the relation:

$$v_d = \mu \tilde{\mathbf{E}}_e \quad (3)$$

where v_d is the drift velocity of the charge carriers and μ is the combined carrier mobility. Substitution of (3) into (2) yields an expression relating $\tilde{\mathbf{E}}_H$ to the carrier mobility and the applied magnetic and electric fields strengths:

$$\tilde{\mathbf{E}}_H = \mu (\tilde{\mathbf{E}}_e \times \tilde{\mathbf{B}}) \quad (4)$$

This equation suggests that the value of μ can be obtained by measuring the value of $\tilde{\mathbf{E}}_H$ upon application of fields E_e and B . In fact, by integrating over the width of the plate, (4) becomes

$$\begin{aligned} V_H &= w\mu E_e B \\ &= w\mu \frac{V_e}{l} B \\ &= \frac{1}{qn} \frac{I_e B}{t} \end{aligned} \quad (5)$$

where V_e is the biasing voltage for fixed voltage measurements and I_e is similar. The fraction on the right-hand side of the latter equation describes the inverse of the charge density of the plate and is referred to as the Hall coefficient, R_H , of a material.

2.2 van der Pauw method

In reality, it is not required to perform both fixed voltage and current measurements to obtain both μ and n as (5) might suggest. By considering the current flow in an infinite lamina and the potentials at several collinear points along it, Leo van der Pauw demonstrated a method of measuring the resistivity and hall coefficient using arbitrarily-shaped, laminar samples, subject to the following conditions [9]:

1. the contacts are sufficiently small,
2. the contacts are on the periphery,
3. the lamella is of uniform thickness and free of holes.

For appropriately prepared samples of known thickness t , with contacts [M,N,O,P], the resistivity can be calculated by measuring the sheet resistance,

$$R_{sh} = \frac{\pi}{\ln(2)} \frac{[R_A + R_B]}{2} f\left(\frac{R_A}{R_B}\right) \quad (6)$$

where R_A and R_B involve swapping the voltage and current contact points. The resistivity of the sample is then simply the product of R_{sh} and t , with the Hall coefficient treated a similar way e.g $R_H = R_{Heff}t$.

The success of this method is, however, subject to the degree to which the samples meet the conditions listed in [2.2]. Van der Pauw laid out an estimation of errors arising from three cases where the positioning and/or size of the sample's contacts do not exactly satisfy the conditions discussed, for a circular disc sample:

Table. The relative errors $\Delta\rho/\rho$ and $\Delta R_H/R_H$ in the calculated values of the resistivity and the Hall coefficient for a circular disc of diameter D on which one contact P is non-ideal, in the senses indicated in the sketches.

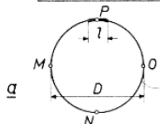
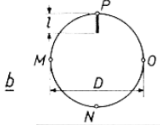
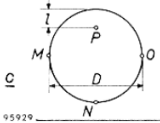
	$\Delta\rho/\rho$	$\Delta R_H/R_H$
	$\approx \frac{-l^2}{16D^2 \ln 2}$	$\approx \frac{-2l}{\pi^2 D}$
	$\approx \frac{-l^2}{4D^2 \ln 2}$	$\approx \frac{-6l}{\pi^2 D}$
	$\approx \frac{-l^2}{2D^2 \ln 2}$	$\approx \frac{-2l}{\pi D}$

Figure 2: Table of errors from van der Pauw's paper, illustrating relative error in ρ and R_H (see [9])

Using conformal mapping, the relative errors can be transformed from the circular geometry to that of a square [[4]]. First, the unit circle, z , in the complex plane is mapped to the positive half-plane via the transformation:

$$u = -i \frac{z+1}{z-1} \quad (7)$$

Then a further transformation is performed mapping u to the unit square, v :

$$v = \frac{1}{k} \int_0^u \frac{dx}{\sqrt{x(1-x^2)}} \text{ where } k \approx 2.62 \quad (8)$$

The relative errors for square samples are discussed in Section 4, Table 6.

3 Method

The pre-fabricated samples were approximately square plates of thickness $t \approx 1-3\mu m$ and area $A \approx 5 \times 5 mm^2$, mounted in a protective casing, with four electrical contacts located at the corners of one side of the plate wired to a 5 pin cable. This cable interfaced to a 4-port bnc terminal box, where the constant-current supply and voltmeter could be connected to the source and sense ports, respectively, in the various configurations required for the measurements.

Properties and measured parameters of InSb, n-type and p-type GaAs				
Sample:	InSB	n-type GaAs	p-type GaAs	units
Type	<i>Intrinsic</i>	<i>Donor dopant</i>	<i>Acceptor dopant</i>	-
Band gap	<i>Indirect</i>	<i>Direct</i>	<i>Direct</i>	-
Sheet resistance	$30.(93) \pm 0.14$	$20.9(2) \pm 0.01$	$110.9(4) \pm 0.01$	Ω
Resistivity	$6.(19) \pm 0.16 \times 10^{-3}$	$6.(28) \pm 0.15 \times 10^{-3}$	$30.(0) \pm 0.9 \times 10^{-3}$	Ωcm^{-1}
Hall coefficient	$-1(84) \pm 19$	$-(5.08) \pm 1.19$	$-1.(57) \pm 0.37$	ΩT^{-1}
Carrier mobility	$5.(95) \pm 0.66 \times 10^4$	$2(430) \pm 540$	$1(41) \pm 33$	$cm^2 V^{-1} s^{-1}$
Carrier density	$1.(63) \pm 0.18 \times 10^{16}$	$3.(93) \pm 0.92 \times 10^{17}$	$1.(41) \pm 0.33 \times 10^{18}$	cm^{-3}

Table 1: Measured parameters of samples

Literature ^a parameters of InSb, n-type and p-type GaAs				
Sample	InSB	n-type GaAs	p-type GaAs	units
Carrier mobility	$\leq 7.7 \times 10^4$	≤ 8500	≤ 400	$cm^2 V^{-1} s^{-1}$
Carrier density	2×10^{16}	4.7×10^{17}	9×10^{18}	cm^{-3}

Table 2: Literature parameters of samples

^asee [5]

The Hall coefficient and resistivity of each sample were obtained using the Van der Pauw method, as described in section 2.2. As a check to confirm the removal of any offset voltage due to the imperfect alignment of the contacts, the resistivity measurements were repeated over the 4 possible permutations, for consistency.

The effective Hall resistance for each sample was calculated using the transverse voltage induced across ten different current values from 0.3-3.0mA at fixed magnetic field strength ranging from 100mT to 300mT. The latter was measured via a magnetic field sensor, placed parallel to the back of the sample so that the reading was representative of that experienced by the sample, regardless of its exact orientation with respect to the magnetic plates (assuming the field was roughly constant over the cross-section of the sample). Due to the possibility of hysteresis in the iron electromagnets affecting the results, the field strength was also measured in steps up to a high value, then measured back down over that range. As illustrated in Figure 3, there was a small degree of hysteresis present at the highest field values, so the field measurements were limited to 300mT, below which no hysteresis was observed.

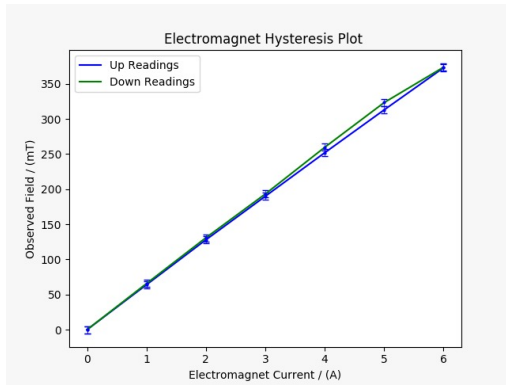


Figure 3: Graph of hysteresis of electromagnetic plates. The effect was considered negligible below 300mT

4 Results & Discussion

The main results are summarised in Table 1, above and figures 4 and 5, below. Details of the error calculations, measurements and numerical fitting for R_H can be found in a set of jupyter notebooks publicly accessible online via Appendix A.

The tabulated parameters in the literature do not provide a precise picture for the individual values of carrier mobility and density, largely owing to the fact that these values depend on many factors, such as temperature, pressure and donor concentration, in addition to each other. The combined values, however, suggest good agreement with the literature (Figures 4,5) for both the InSb and GaAs n-type samples - in the latter cases, indicating a likely dopant concentration somewhere between 2-5 times that of the intrinsic carrier.

Of note is the very large Hall co-efficient of the non-doped InSb, which was negative in sign. This can be explained by the relative values of its intrinsic carrier mobilities: $10^4 cm^2 V^{-1} s^{-1}$ for electrons, compared to $10^2 cm^2 V^{-1} s^{-1}$ for holes [5]. At $T=300K$, the lifetime of both holes and electrons is the same $\tau_n = \tau_p \approx 5 \times 10^{-8} s$ [5], so from equation 9,

$$\mu = \frac{q\tau}{m} \quad (9)$$

where m is the effective mass of the carrier, we can see that the holes have a much larger effective mass compared to the electrons in InSb. This heavily weights the current density according to the number of electrons, which therefore become the dominant carrier type:

$$\begin{aligned} \tilde{\mathbf{J}}_{\text{drift}} &= (qn\mu_n + qp\mu_p) \tilde{\mathbf{E}} \\ &\approx qn\mu_n \tilde{\mathbf{E}} \quad \text{when } \mu_n/\mu_p \gg 1 \end{aligned}$$

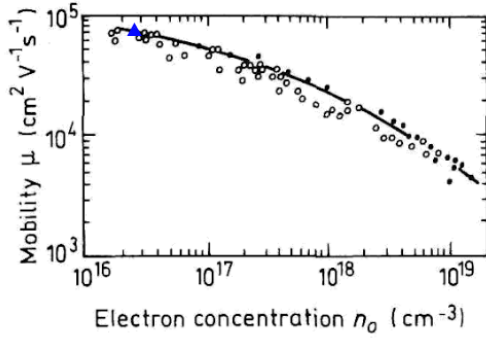


Figure 4: Observed values for carrier mobility vs (majority) carrier density, at STP conditions, for InSb [6]. Blue triangle represents measured value.

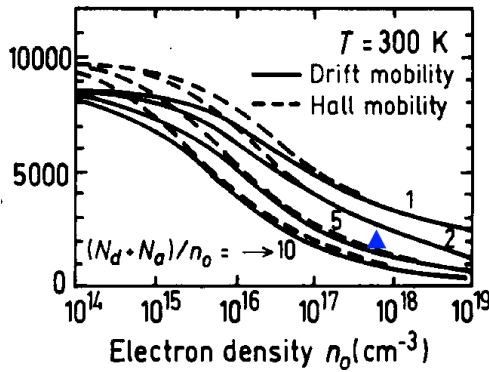


Figure 5: Observed values for carrier mobility vs (majority) carrier density, at STP conditions, for GaAs [8]. Blue triangle represents measured value.

Four out of the five measured parameters in Table 1 were affected by a considerable degree of uncertainty resulting from the imperfect nature of the samples. With the exception of the sheet resistance (the only dimensionless or dimension independent parameter), all other parameters were subject to measurement errors incurred as a result of the samples not meeting two of the necessary conditions required for the van der Pauw technique, namely that:

- there must be four contact leads attached...along the edge of the sample, and
- these leads must be pointlike in size

In the absence of these conditions, the measured values are subject to relative errors that depend on the geometry of the sample. Using conformal mapping, it can be calculated (see [4]) that the relative error in ρ and R_H are as described below (Table 6)

Sample	-	InSB	n-type GaAs	p-type GaAs
$\frac{d}{D}$	-	1 / 6.0	1.5 / 6.5	1.5 / 6.5
$\frac{\Delta\rho}{\rho}$	$-8.5 \left(\frac{d}{D}\right)^4$	$-4.8E^{-3}$	-0.024	-0.024
$\frac{\Delta R_H}{R_H}$	$-4.4 \left(\frac{d}{D}\right)^2$	-0.10	-0.23	-0.23

Figure 6: Relative error due to contacts

For the parameters associated with R_H , the relative errors due to contact size/placement were much larger than those related to the measurements (see Appendix A), due to the quadratic dependence on the ratio of the contacts to the sample itself.

5 Conclusion

In this investigation, the van der Pauw technique was used to measure the Hall coefficient and sheet resistance of three semiconductors. From these values, the carrier mobility and density was calculated for each sample and compared to the literature. The errors associated with both the measurements and the placement and size of contacts on the sample were considered, which suggest that a more precisely fabricated sample, specifically with a smaller contact size to sample length ratio, ideally less than 0.048 [4], would achieve a relative error of less than 1%.

Word count: 2527 words

References

- [1] M. Andersson, A. Lloyd Spetz, and R. Pearce. 4 - recent trends in silicon carbide (sic) and graphene-based gas sensors. In Raivo Jaaniso and Ooi Kiang Tan, editors, *Semiconductor Gas Sensors*, Woodhead Publishing Series in Electronic and Optical Materials, pages 117 – 158. Woodhead Publishing, 2013.
- [2] Bernd Ebenhoch, Stuart A.J. Thomson, Kristijonas Genevius, Gytis Juka, and Ifor D.W. Samuel. Charge carrier mobility of the organic photovoltaic materials ptb7 and pc71bm and its influence on device performance. *Organic Electronics*, 22:62 – 68, 2015.
- [3] Grard Ghibaudo and Quentin Rafhay. *Electron and Hole Mobility in Semiconductor Devices*, pages 1–13. American Cancer Society, 2014.
- [4] Daniel W. Koon. Effect of contact size and placement, and of resistive inhomogeneities on van der pauw measurements. *Review of Scientific Instruments*, 60(2):271–274, 1989.
- [5] M. Levinshstein. *Handbook Series on Semiconductor Parameters*. Number v. 1 in Handbook series on semiconductor parameters. World Scientific, 1997.
- [6] E Litwin-Staszewska, W Szymańska, and R Piotrkowski. The electron mobility and thermoelectric power in insb at atmospheric and hydrostatic pressures. *physica status solidi (b)*, 106(2):551–559, 1981.
- [7] R.S. Popovic. *Hall Effect Devices, Second Edition*. Series in Sensors. CRC Press, 2003.
- [8] D.L. Rode. Chapter 1 low-field electron transport. volume 10 of *Semiconductors and Semimetals*, pages 1 – 89. Elsevier, 1975.
- [9] LV Van der Pauw. A method of measuring specific resistivity and hall effect of discs of arbitrary shape. *Philips research reports*, 13:1–9, 1958.

- [10] N. Yamazoe and K. Shimano. 1 - fundamentals of semiconductor gas sensors. In Raivo Jaanisoo and Ooi Kiang Tan, editors, *Semiconductor Gas Sensors*, Woodhead Publishing Series in Electronic and Optical Materials, pages 3 – 34. Woodhead Publishing, 2013.

A Data

<https://github.com/TomFahey/Hall-Effect-Lab-Data>